

# The Fate of Planets

Eva Villaver

*Universidad Autónoma de Madrid, Dpto. Física Teórica, Módulo 15, Facultad de Ciencias,  
Campus de Cantoblanco, 28049 Madrid, Spain. e-mail: eva.villaver@uam.es*

**Abstract.** As a star evolves off the Main Sequence, it endures major structural changes that are capable of determining the fate of the planets orbiting it. Throughout its evolution along the Red Giant Branch, the star increases its radius by two orders of magnitude. Later, during the Asymptotic Giant Branch, it loses most of its initial mass. Finally, during the Planetary Nebulae phase, it emits intense radiation before ultimately beginning its fade as a white dwarf. We show how the several competing processes (stellar mass-loss, gravitational and frictional drag, tidal forces, planet accretion and evaporation) affect the survival of planets around evolved stars.

**Keywords:** Planets, Evolved Stars, Giant and White Dwarf stars

**PACS:** 97.82.j, 97.10.Me, 97.20.Li

## PLANET'S FATE BEYOND THE MAIN SEQUENCE

### The Red Giant Branch Phase

Once the nuclear burning has been exhausted in the core, low- and intermediate mass stars evolve into the Red Giant Branch (RGB) phase. During the RGB, hydrogen burning continues in a shell outside the helium core, which now, devoid of energy sources, is contracting and heating up. The stellar evolution timescales (in the absence of significant mass loss) are set by the rate of consumption of the nuclear fuel. As the core contracts the envelope expands and cools. The stellar effective temperature decreases while the star's radius and luminosity increase.

There are several competing processes that affect the orbital distance between the star and the planet as the star evolves off the Main Sequence (MS): the changes in the mass of both the planet and the star ( $\dot{M}_p$  and  $\dot{M}_*$  respectively), the gravitational and frictional drag ( $F_g$  and  $F_f$ ), and the tidal force. To determine the rate of change in the planet's orbit  $a$  we consider a planet of mass  $M_p$  and radius  $R_p$  moving with a velocity,  $v$ , in a circular orbit ( $e = 0$ ) around a star of mass  $M_*$ . The conservation of angular momentum gives the equation for the rate of change in the orbital radius of the planet (see, e.g., Alexander et al. 1, Livio & Soker 24, Villaver & Livio 50),

$$\left(\frac{\dot{a}}{a}\right) = -\frac{\dot{M}_* + \dot{M}_p}{M_* + M_p} - \frac{2}{M_p v} [F_f + F_g] - \left(\frac{\dot{a}}{a}\right)_t, \quad (1)$$

where  $(\dot{a}/a)_t$  is the rate of orbital decay due to the tidal interaction.

It has been shown that for giant stars, which have massive convective envelopes, the most efficient mechanism to produce tidal friction is turbulent viscosity [e.g., 53, 54, 55]. The dissipation timescale is determined by the effective eddy viscosity, with eddy

**TABLE 1.** Minimum Orbital Radius to Avoid Tidal Capture

$M_*$	$R_*^{\max}$ [AU]	$a_{\min}$ [AU]		
		$M_p = M_J$	$M_p = 3 M_J$	$M_p = 5 M_J$
1 $M_\odot$	1.10	3.00	3.40	3.70
2 $M_\odot$	0.84	2.10	2.40	2.50
3 $M_\odot$	0.14	0.18	0.23	0.25
5 $M_\odot$	0.31	0.45	0.55	0.60

velocities and length scales given approximately by standard mixing length theory if convection transports most of the energy flux [55, 46, 33]. The tidal term is given by

$$\left(\frac{\dot{a}}{a}\right)_t = \frac{f}{\tau_d} \frac{M_{\text{env}}}{M_*} q (1+q) \left(\frac{R_*}{a}\right)^8, \quad (2)$$

with  $M_{\text{env}}$  being the mass in the convective envelope,  $q = M_p/M_*$ , and  $\tau_d$  the eddy turnover timescale, given in the case of a convective envelope [33],

$$\tau_d = \left[ \frac{M_{\text{env}} (R_* - R_{\text{env}})^2}{3L_*} \right]^{1/3}, \quad (3)$$

where  $R_{\text{env}}$  is the radius at the base of the convective envelope. The term  $f$  in Eq. (2) is a numerical factor obtained from integrating the viscous dissipation of the tidal energy across the convective zone. [55] used  $f = 1.01(\alpha/2)$  where  $\alpha$  is the mixing length parameter. [46] confirmed that observations are consistent with  $f \approx 1$  as long as  $\tau_d \ll P$  with  $P$  being the orbital period. We therefore used  $f = (P/2\tau_d)^2$  to account only for the convective cells that can contribute to viscosity when  $\tau_d > P/2$ , otherwise we take  $f = 1$ . It is important to note here that the initial value of the eccentricity has little effect on the orbital decay rate [e.g., 17].

In Fig. 1 we show the orbital evolution for 4 different initial orbital radius and for planets orbiting stars with MS masses of 2 and 3  $M_\odot$ , solar metallicity, and a mass-loss prescription with a Reimers parameter of  $\eta_R = 0.6$  [35]. The figure demonstrates the three possible outcomes of orbital evolution for a Jupiter mass planet along the RGB [50]: (i) Beyond a certain initial orbital separation, the orbital separation simply increases, due to systemic mass loss. (ii) There is a range of initial orbital separations in which the orbit decays, but the planet avoids being engulfed. (iii) Inward from some critical, initial orbital separation, the planet is engulfed mostly due to tidal interaction. Note that tidal interaction along the RGB phase can determine a planet's fate even at large distances beyond the stellar radius.

It is important to mention that the stellar structure enters into the calculation of the tidal term. For the calculations presented here we have used stellar models provided to us by Lionel Siess. These were calculated based on the stellar evolution code STAREVOL described in [40].

In Fig. 2, the top panel shows the evolution along the RGB of a 3  $M_\odot$  star on the HR diagram. The bottom panel shows the orbital evolution for a planet with mass

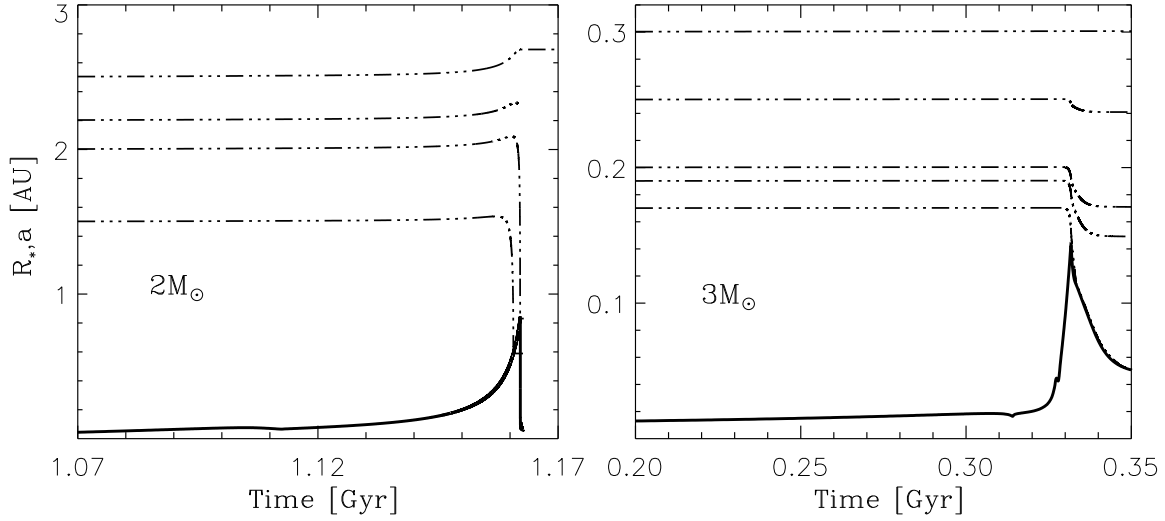


**FIGURE 1.** Evolution of the orbital separation of a planet with Jupiter’s mass (dash-dotted line) compared with the evolution of the stellar radius (solid line) along the Red Giant Branch phase. The panel on the left is for a star with a main sequence mass of  $2 M_{\odot}$  and the panel on the right for a  $3 M_{\odot}$  star. The evolution of the orbital distance is shown for different initial orbits.

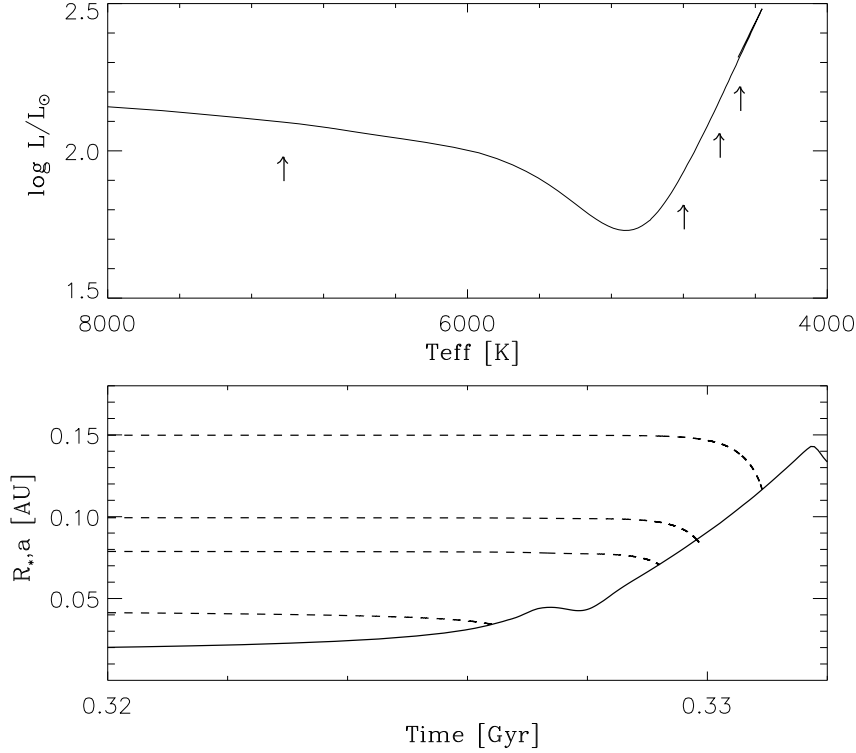
$5 M_J$  (dash-dotted line) together with the evolution of the stellar radius (solid line). We selected small initial orbits to identify at which points during the RGB these planets are swallowed by their stars (marked by the location of the arrows).

Table 1 summarize some of our results, where we list the minimum initial orbital distance for which a planet with a given mass avoids being engulfed by the star. The second column gives the maximum radius reached by the star on the RGB,  $R_*^{\max}$  (in AU), and the following columns give the minimum orbital distances (in AU) at which planets with masses of 1, 3, and  $5 M_J$  (respectively) avoid being engulfed.

For all the initial orbits that satisfy the condition  $a_o \leq R_*^{\max}$  the planet gets engulfed by the star at same point before the end of the RGB phase. The more massive the planet the stronger is the tidal interaction with the star, and therefore the sooner the orbit decays to meet the stellar radius.

We would like to highlight that the tidal “capture” radius increases with the planet’s mass; a Jupiter-mass planet is captured by a  $2 M_{\odot}$  star if it starts at an initial orbit of 2.1 AU while a  $5 M_J$  planet will be engulfed by the star if it has an initial orbit  $a_o < 2.5$  AU. Moreover, the tidal capture radius decreases with increasing stellar mass; for a  $5 M_J$  planet the initial orbit has to be larger than  $a_o \approx 3 \times R_*^{\max}$  to avoid tidal capture around a  $2 M_{\odot}$  star, while it has to be larger than  $a_o \approx 2 \times R_*^{\max}$  to avoid tidal capture around a  $M_{\odot}$  star.

At large distances from the star, the densities involved are low, and the drag terms associated with the forces  $F_f$  and  $F_g$  in Eq. (1) play a negligible role in the evolution of the orbit. Moreover, since the accretion rate onto the planet is always small compared to the stellar mass-loss rate, the first term in Eq. (1) is dominated by  $\dot{M}_*$ . The temporal behavior of the orbit is then mostly governed by the relative importance of the terms



**FIGURE 2.** The top panel shows the evolution of a  $3 M_{\odot}$  star along the Red Giant Branch phase on the HR diagram. The bottom panel shows the same as the right panel of Fig. 1 but for  $5 M_{\text{J}}$  planets with different initial orbital separations. The arrows show the location on the HR diagram at which the planet enters the stellar envelope. The evolution of the stellar radius is shown as a solid line on the bottom panel.

associated with the stellar mass-loss  $\dot{M}_{*}$  and the tidal interaction  $(\dot{a}/a)_t$ . Note also that the peak RGB mass-loss rates are higher for lower-mass stars, and the lowest mass stars also reach the largest radius at the tip of the RGB.

Red giant mass-loss rates are somewhat uncertain. It is important to emphasize that (for the work presented here) we have estimated the mass-loss rate using the Reimers prescription with  $\eta_R = 0.6$ . This seems to reproduce fairly well the observations of individual RGB stars. Uncertainties in both stellar evolution and mass-loss will directly influence the planet's survival, a different set of evolutionary models using different mass-loss rates will change the planet's fate. An increase in stellar mass-loss will move the orbit outwards to the point where tidal forces are no longer effective. Higher mass-loss will also have the effect of decreasing the evolutionary timescales during this phase and might influence as well the maximum stellar radius.

## The Asymptotic Giant Branch Phase

The major structural changes in the post-main sequence evolution of low- and intermediate-mass stars occur during the RGB and Asymptotic Giant Branch (AGB) phases. During the RGB and AGB the stellar effective temperature is always lower than its main sequence value and therefore it has no influence on the planet's survival. However, it is during the late AGB evolution, the so-called thermal-pulsing AGB phase, that a planet's orbit will be most influenced, since during this phase the star loses most of its initial mass and reaches its maximum radius.

If a planet becomes engulfed by the stellar envelope (it could be along the RGB or the AGB phase) it can spiral-in and evaporate totally; or it can accrete mass and become a close low-mass companion to the star. It is important to mention that even if a planet gets inside the stellar envelope it may survive under certain conditions. In [49] we give an estimate of the maximum planet mass that can be evaporated inside an AGB envelope,  $0.014 M_{\odot}$  or  $15 M_J$ . This estimate is very uncertain given it was obtained by equating the location of the evaporation region (where the local sound speed in the stellar envelope matches the escape velocity from the planet's surface) to the energy required to expel the envelope [44, 45, 27]. The value of this maximum mass is very debatable because it depends on several factors, such as the efficiency of envelope ejection [31], which are largely unknown.

The structural changes that an AGB star undergoes in response to the dissipation of a planet in its interior are complex and have been extensively explored by [41, 42]. So far the details of the destruction of such a planet within the stellar envelope of an AGB star have not been studied in detail.

The final orbit reached by the planet at the end of the AGB phase is simply related to the stellar initial-to final mass relation for planets in orbits that *avoid* engulfment along the AGB phase. The initial mass of the star, the higher the amount of mass lost during the AGB phase and hence the larger the planet's orbital expansion. Planets reach a final orbital distance at the end of the AGB phase, determined by multiplying the initial orbit by  $M_*/M_{WD}$  where  $M_{WD}$  is the white dwarf mass. The orbital expansion factors for white dwarf progenitor stars are given in [49].

Another effect to consider is whether the planet becomes unbound due to the change in mass of the central star. Unbinding can be expected if the stellar mass-loss timescale,  $\tau_{mass-loss}$ , satisfies  $\tau_{mass-loss} < \tau_{dyn}$ , where  $\tau_{mass-loss}$  is given by

$$\tau_{mass-loss} \sim \frac{M_*}{\dot{M}_*} \quad (4)$$

and the dynamical timescale,  $\tau_{dyn}$ , by

$$\tau_{dyn} \sim \left[ \frac{r^3}{G(M_* + M_p)} \right]^{1/2}, \quad (5)$$

with  $\dot{M}_*$  being the stellar mass-loss rate,  $M_p$  the planet's mass, and  $G$  the gravitational constant. Given that  $\tau_{dyn} \sim 50$  yr while the shortest mass-loss timescale is  $\tau_{mass-loss} \sim 10^5$  yr, it is very unlikely that a planet will become unbound due to the decrease in the stellar mass during the AGB phase.

Therefore, the orbit of the planet will expand due to the heavy stellar mass-loss rates experienced during the AGB evolution if the planet has avoided being engulfed during both the RGB and AGB phases. Larger differences between the initial and final mass of the star are experienced for the more massive progenitors, causing the orbits of planets orbiting the more massive stars (note that we are always referring to stars in the 1–5  $M_{\odot}$  mass range for which complete stellar evolution models exist) to be modified by the larger factors (up to 5.5 times larger than the initial orbit).

## **The Planetary Nebulae Phase**

During the post-main sequence evolution of the star the stellar effective temperature always remains lower than its main sequence value. However, once the star leaves the AGB phase, the high mass-loss rate ceases and the remnant core moves in the HR diagram at constant luminosity toward higher effective temperatures into the Planetary Nebulae (PN) stage, before the star reaches the white dwarf (WD) cooling track. The planet's orbit is not expected to change further at this stage. However, the main processes responsible for shaping PNe (high velocity winds) and powering PNe line emission (high stellar effective temperatures) need to be considered to establish the survival of a planet during this phase.

The luminosity, mass, and timescale of evolution of the star during the PN phase depend mostly on the stellar core mass. The stellar luminosity during this phase is within the range  $3.5$  to  $23 \times 10^3 L_{\odot}$  (for the lowest  $0.56$  and highest  $0.9 M_{\odot}$  mass remnant, respectively) and the stellar temperature can reach  $100\,000$ – $380\,000$  K (for the same core masses, respectively). The hydrogen ionizing photon flux, which is of the order of  $10^{48} \text{ s}^{-1}$  [48, 47], is responsible for the PNe ionized line emission. PNe central stars also emit very high velocity winds (with speeds of a few thousands of  $\text{km s}^{-1}$ ) which are driven by the transfer of photon momentum to the gas, through absorption by strong resonance lines. The PN is largely shaped by the interaction of this high velocity wind with the slowly ejected material during the AGB phase. The survival of a gas planet as the star evolves into the PN phase strongly depends on the planet's surface temperature, which ultimately determines whether or not high evaporation rates are set at the planet's surface.

### *Planet's Evaporation Rates*

As a consequence of the high temperatures reached at the planet's upper atmosphere it is expected that an outflow will develop due to the absorption of the XUV radiation. High temperatures can cause the outer layers of the planet to escape rapidly. Note that at the orbital distances considered, the planet will be well within the typical inner radius of the nebular shell ( $0.01$  to  $0.1 \text{ pc}$ ) [48] and therefore a decrease in the photon flux arriving at the planet's surface due to absorption by the nebula is not expected.

The problem of a general outflow from a stellar (or planetary) body can be described with the same set of equations used by [30] to describe the solar wind. Although a

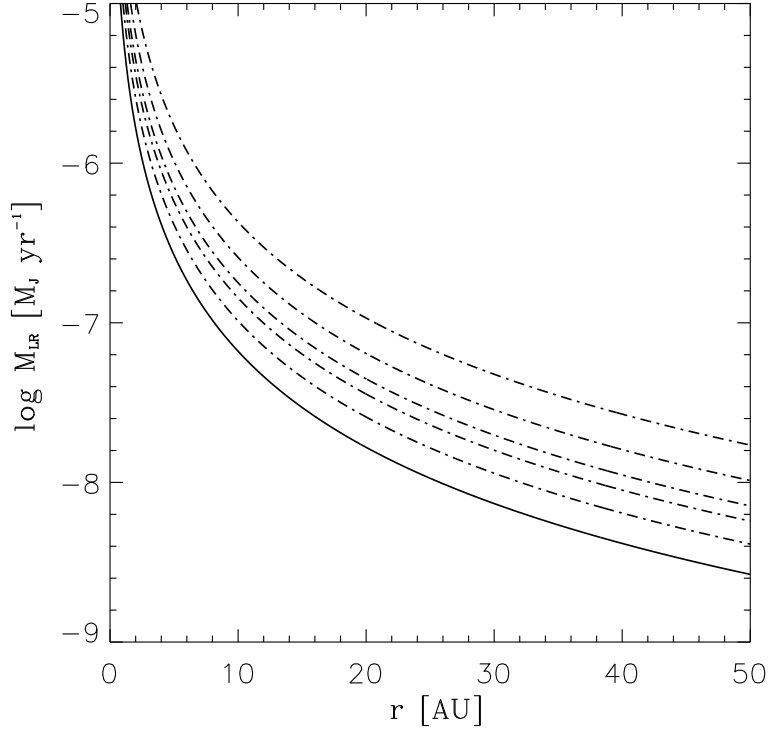


**FIGURE 3.** Mass-loss in logarithmic scale and  $M_{\text{Jyr}}^{-1}$  vs. orbital distance of a Jupiter-like planet under hydrodynamic escape conditions. The different lines are for stellar MS masses 1, 1.5, 2, 2.5, 3.5 and 5  $M_{\odot}$ . The radiation field for the star has been taken at 30,000 yr after the star enters the Planetary Nebulae phase.

complete treatment of the evaporative wind requires the integration of the energy, mass, and momentum transfer equations, we can estimate the outflowing particle flux  $\Phi_H$  (e.g. Watson et al. 51) by equating the energy input  $(\epsilon L_{\text{XUV}}/4) \times (R_1/a)^2$  to the energy required for hydrogen to escape  $GM_p m_H/R_p$ , giving

$$\Phi_H \simeq \frac{\epsilon L_{\text{XUV}} R_1^2 R_p}{4a^2 GM_p m_H} \quad (6)$$

where  $R_1$  is the planet's radius where most of the XUV radiation is absorbed, defined as the level where the optical depth is unity,  $a$  is the orbital distance,  $R_p$  and  $M_p$  are the planet's radius and mass respectively and  $\epsilon L_{\text{XUV}}$  the fraction of the stellar XUV luminosity that is converted into thermal energy. The most uncertain parameter in Eq. 6 is  $R_1$ , or  $\xi = R_1/R_p$ , since its determination requires the full solution of the hydrodynamical escape problem with radiation transfer in a strongly externally heated atmosphere. Generally, simulations produce higher escape rates than the ones given by Eq. 6 for  $\xi = 3$  as the density increases. This is the result of the higher total amount of energy absorbed in an extended atmosphere, as opposed to that absorbed in a single

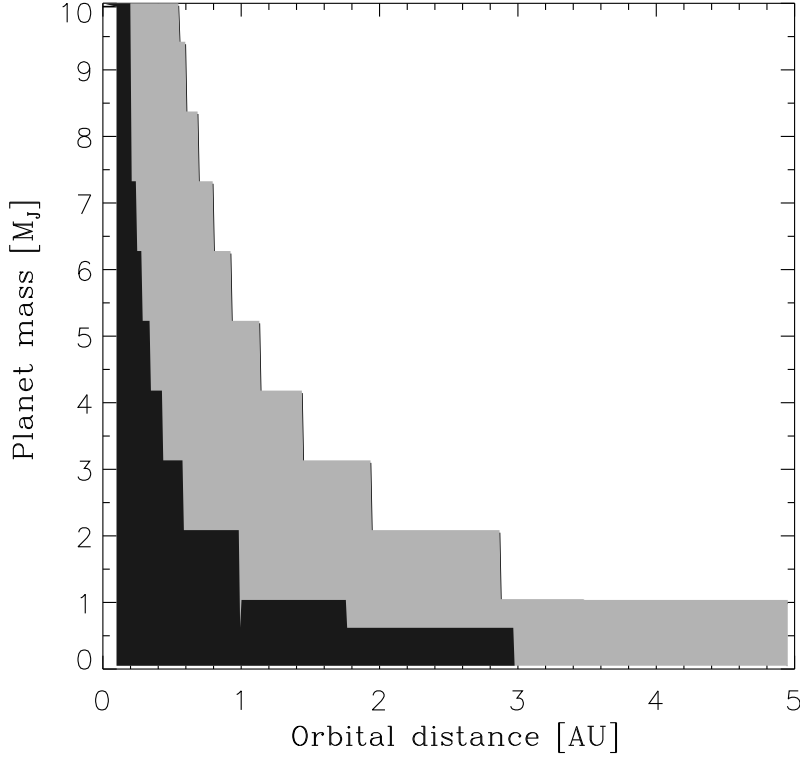


**FIGURE 4.** The dark-gray area represent the region where a gas planet loses 50% of its mass when orbiting a  $0.56 M_{\odot}$ . The same is for the light-gray area but using a different parameter for the calculation of evaporation rates.

layer (the approximation used to obtain Eq. 6; see Villaver & Livio 49).

The mass-loss rates (obtained by using  $\xi = 3$  in Eq. 6) from a  $1 M_J$  planet for central stars (at 36 000 K) with different masses are plotted in Fig. 3, versus the orbital distance. The different lines account for the different central star masses considered, with the mass-loss rates increasing with the stellar mass.

It is important to note that none of the calculations in the literature for exoplanets orbiting MS solar-mass stars includes heating rates as high as the ones expected for a planet orbiting a PN central star, and as it has been shown the inclusion of X-ray irradiation from the star strongly increases the heating in planetary exospheres. The mass-loss rates given in Fig. 3 should be considered merely as order of magnitude approximations to the actual mass-loss rates from a planet exposed to a PN central star. In addition, it is very likely that the planet will inflate as radiation is transformed into heat inside its atmosphere, which will lead to further increase in the planet's evaporation rate with our approach. An appropriate determination of the escape rate will require a solution of the hydrodynamic escape equations for the case under consideration.

In Fig. 4 we show the region (on the planet mass versus orbital distance plane) inside which Jupiter-like planets will be destroyed, as the star evolves into the white dwarf



phase orbiting a  $0.56 M_{\odot}$  star (which correspond to  $1 M_{\odot}$  main sequence mass). The dark gray and gray shaded areas (computed for  $\xi=3$  and 10 respectively, see Villaver & Livio 49) represent the regions for which planets will lose 50 % of their mass before the star enters the white dwarf cooling track due to the evaporation caused by thermal heating. Note that the region for which the planet will undergo total evaporation due to thermal heating is inside the AGB stellar radius for the  $0.9 M_{\odot}$  white dwarf.

## PLANETS OBSERVED AROUND EVOLVED STARS

### *Giant stars*

To date, the frequency of planets around massive stars can only be determined by searching stars that have left the MS. In only a few years Doppler techniques applied to sub-giants and clump giants has succeeded in discovering more than 40 planets around stars with masses between 1.2 and  $4 M_{\odot}$  [4, 5, 8, 12, 13, 14, 18, 19, 20, 23, 25, 28, 29, 34, 36, 37, 38, 39].

Despite the small number statistics these surveys have revealed important clues about the planet distribution among the more massive evolved stars. First, it seems that there is a deficiency of close-in planets orbiting evolved stars with masses  $M > 1.3 M_{\odot}$  [19, 37, 52] despite the fact that these planets are found around  $\approx 20$  % of the MS stars with  $\approx 1 M_{\odot}$ . Second, the frequency of planets seems also to be higher around intermediate-mass stars [25, 19].

In [50] we show that stellar evolution could explain the observed distribution of the semi-major axes of planetary orbits around evolved stars (i.e., semi-major axis  $> 0.5$  AU). Despite the uncertainties in stellar (and tidal) evolution theory when the details of the orbital evolution are accurately calculated, tidal interactions constitute a quite powerful mechanism, capable of capturing close-in planets into the envelope of evolved stars.

### *White dwarfs*

Low-mass brown dwarfs and extrasolar planets in wide orbits around white dwarfs would have temperatures lower than 500 K and therefore could be detected via direct imaging in the Infrared [3]. Infrared searches for planets around white dwarfs (e.g. Mullally et al. 26, Gould et al. 11, Farihi et al. 6, Hogan et al. 16) are underway. From these surveys it has been found that approximately 2 % of all white dwarfs with cooling ages  $\leq 0.5$  Gyr show evidence of an infrared excess [7].

Moreover, disks formed by the tidal disruption of an asteroid have been proposed to explain the high anomalous photospheric-metal abundances found in some white dwarfs [2, 21, 9]. Furthermore, there are more than a dozen white dwarfs known to host circumstellar debris disks (e.g. [7, 9, 21]).

Planets around white dwarfs with masses  $M_{WD} \geq 0.7 M_{\odot}$  (that formed from single stars with masses  $M_{MS} \geq 2.5 M_{\odot}$ ), are generally expected to be found at orbital radii  $r$

$\geq 15$  AU due to the effects of mass-loss on the AGB phase [49]. The sensitivity of the current surveys at such larger distances from the star has to be further explored.

### *Planets and sdB stars*

Among the planets found orbiting evolved stars, there are several systems that beg further investigation: e.g. the planet of mass  $3.2 M_J$  with an orbital separation of 1.7 AU orbiting the extreme horizontal branch star V391 Pegasi [43]. The star V391 Pegasi lost its hydrogen-rich envelope (for reasons that are not well understood) at the end of the Red Giant Branch leaving behind a hot B-type sub-dwarf (sdB) with a surface temperature of 30,000 K.

More recently, [10] has found a planet orbiting the sdB HD 149382 at a distance of only about five solar radii. At that distance, the planet must have survived engulfment in the red giant envelope.

Serendipitous discoveries of two substellar companions around the eclipsing sdB binary HW Vir at distances of 3.6 AU and 5.3 AU (Lee et al. 2009) and one brown dwarf around the similar system HS 0705+6700 with a separation of  $< 3.6$  AU [32] followed recently. It seems more than plausible that the presence of a planetary companion can trigger envelope ejection and enabled the sdB star to form. Hot sub-dwarfs have been identified as the sources of the unexpected ultraviolet (UV) emission in elliptical galaxies, but the formation of these stars is not fully understood (see e.g. Heber 15).

## **SUMMARY**

The conditions for planet survival as the star evolves off the main sequence depend on the initial mass of the star. Most of the MS close-in planets will most likely be destroyed as they get engulfed by the star during the RGB and AGB phase. As the star leaves the AGB and enters the PN phase, high effective temperatures at very high luminosities set up an evaporation flux at the surface of the planet. At certain orbital distances the evaporation rates are high enough to cause a total destruction of the planet. By integrating the evaporation rates as the star evolves during the PN into the white dwarf cooling track, Jupiter-like planets will be destroyed if they remain at orbital distances  $r \leq 5$  AU from a low mass white dwarf ( $M_{WD} \leq 0.63 M_{\odot}$ ) and large planet ablation is expected up to 10 AU. In particular, Jupiter in our own Solar system is barely expected to survive. More massive stars evolve very fast during the PN phase and do not maintain high evaporation rates long enough to cause planet destruction, unless the planets were to be found at small orbital distances ( $r \leq 2.5$  AU). However, we have shown that planets orbiting the more massive PN central stars cannot be found at small orbital distances: if a planet orbiting a  $0.9 M_{\odot}$  progenitor is to survive AGB engulfment then its orbit has to be beyond  $r \geq 29$  AU.

We find that the evolution of the star alone can quantitatively explain the observed lack of close-in planets around evolved stars even allowing for the uncertainties associated with mechanisms such as mass loss along the RGB or tidal-interaction theory. Along similar lines, since we find a high probability of tidal capture of the planet by evolved

stars, the higher frequency of planets observed around intermediate-mass stars [25, 19] seems to imply that the efficiency of planet formation must be considerably higher for more massive stars, compared to their solar analogous.

## REFERENCES

1. Alexander, M. E., Chau, W. Y., & Henriksen, R. N. 1976, *ApJ*, 204, 879
2. Becklin E. E. et al. 2005, *ApJ*, 632, L119
3. Burleigh M. R., Clarke F. J., Hodgkin S. T., 2002, *MNRAS*, 331, L41
4. Döllinger, M. P., Hatzes, A. P., Pasquini, L., Guenther, E. W., Hartmann, M., Girardi, L., & Esposito, M. 2007, *A&A*, 472, 649
5. Döllinger, M. P., Hatzes, A. P., Pasquini, L., Guenther, E. W., Hartmann, M., & Girardi, L. 2009, *A&A*, 499, 935
6. Farihi J., Becklin E. E., Zuckerman B., 2008, *ApJ*, 681, 1470; Farihi J., 2009, *MNRAS*, 398, 2091
7. Farihi, J., Jura, M., & Zuckerman, B. 2009, *ApJ*, 694, 805
8. Frink, S., Mitchell, D. S., Quirrenbach, A., Fischer, D. A., Marcy, G. W., & Butler, R. P. 2002, *ApJ*, 576, 478
9. Gänsicke B. T. 2008, *MNRAS*, 391, L103
10. Geier et al. 2009, *ApJ*, 702, L99
11. Gould A., Kilic M., 2008, *ApJ*, 673, L75
12. Hatzes, A. P., Cochran, W. D., Endl, M., McArthur, B., Paulson, D. B., Walker, G. A. H., Campbell, B., & Yang, S. 2003, *ApJ*, 599, 1383
13. Hatzes, A. P., Guenther, E. W., Endl, M., Cochran, W. D., Döllinger, M. P., & Bedalov, A. 2005, *A&A*, 437, 743
14. Hatzes, A. P., et al. 2006, *A&A*, 457, 335
15. Heber, U. 2009, *ARA&A*, 47, 211
16. Hogan, E., Burleigh, M.R., & Clarke, F. J. 2009, *MNRAS*, 396, 2074
17. Jackson, B., Greenberg, R., & Barnes, R. 2008, *ApJ*, 681, 1631
18. Johnson, J. A., et al. 2007, *ApJ*, 665, 785
19. Johnson, J. A., et al. 2007, *ApJ*, 670, 833
20. Johnson, J. A., Marcy, G. W., Fischer, D. A., Wright, J. T., Reffert, S., Kregenow, J. M., Williams, P. K. G., & Peek, K. M. G. 2008, *ApJ*, 675, 784
21. Kilic et al. 2005, *ApJ*, 632, L115;
22. Kilic M., Gould A., Koester D., 2009, *ApJ*, 705, 1219
23. Liu, Y. J., et al. 2007, *ApJ*, 672, 553
24. Livio, M. & Soker, N. 1984, *MNRAS*, 208, 763
25. Lovis, C. & Mayor, M. 2007, *A&A*, 472, 657
26. Mullally F. et al. 2008, *ApJ*, 676, 573
27. Nelemans, G., & Tauris, T. M. 1998, *A&A*, 335, L85
28. Niedzielski, A., et al. 2007, *ApJ*, 669, 1354
29. Niedzielski, A., Nowak, G., Adamów, M., & Wolszczan, A. 2009, arXiv:0906.1804
30. Parker, E. N. 1963, *Interplanetary Dynamical Processes*, New York, Wiley, 51-91
31. Portegies Zwart, S. F., & Yungelson, L. R. 1998, *A&A*, 332, 173
32. Qian, S.-B. et al. 2010, *MNRAS*, 401, 34
33. Rasio, F. A., Tout, C. A., Lubow, S. H., & Livio, M. 1996, *ApJ*, 470, 1187
34. Reffert, S., Quirrenbach, A., Mitchell, D. S., Albrecht, S., Hekker, S., Fischer, D. A., Marcy, G. W., & Butler, R. P. 2006, *ApJ*, 652, 661
35. Reimers, D. 1975, *Men. Soc. Roy. Sci. Liège*, 6th Ser. 8, 369
36. Sato, B., et al. 2007, *ApJ*, 661, 527
37. Sato, B., et al. 2008, *PASJ*, 60, 539
38. Setiawan, J., et al. 2003, *A&A*, 398, L19
39. Setiawan, J., et al. 2005, *A&A*, 437, L31
40. Siess, L. 2006, *A&A*, 448, 717
41. Siess, L. & Livio, M. 1999a, *MNRAS*, 304, 925

42. Siess, L. & Livio, M. 1999b, MNRAS, 308, 1133
43. Silvotti, R. et al. 2007, Nature, 449, 189
44. Soker, N. 1996, ApJL, 460, L53
45. Soker, N. 1998, AJ, 116, 1308
46. Verbunt, F. & Phinney, E. S. 1995, A&A, 296, 709
47. Villaver, E., García-Segura, G. & Manchado, A. 2002, ApJ, 571, 880
48. Villaver, E., Manchado, A., & García-Segura, G. 2002b, ApJ, 581, 1204
49. Villaver, E. & Livio, M. 2007, ApJ, 661, 1192
50. Villaver, E. & Livio, M. 2009, ApJL, 705, L81
51. Watson, A. J., Donahue, T. M., & Walker, J. C. G. 1981, Icarus, 48, 150
52. Wright, J. T., Upadhyay, S., Marcy, G. W., Fischer, D. A., Ford, E. B., & Johnson, J. A. 2009, ApJ, 693, 1084
53. Zahn, J. P. 1966, Annales d'Astrophysique, 29, 489
54. Zahn, J.-P. 1977, A&A, 57, 383
55. Zahn, J.-P. 1989, A&A, 220, 112